Supramolecular Organometallic Polymer Chemistry: Multiple Morphologies and Superstructures from the Solution Self-Assembly of Polyferrocene-*block*-Polysiloxane-*block*-Polyferrocene Triblock Copolymers

Rui Resendes, Jason A. Massey, Karen Temple, Lan Cao, K. Nicole Power-Billard, Mitchell A. Winnik,* and Ian Manners*[a]

Abstract: The solution self-assembly of an organometallic – inorganic triblock copolymer, poly(ferrocenyldimethylsilane)-*block*-poly(dimethylsiloxane)-*block*-poly(ferrocenyldimethylsilane) (PFDMS-*b*-PDMS-*b*-PFDMS, **3b**; block ratio 1:13:1; $M_n = 2.88 \times 10^4$ g mol^{-1}, polydispersity (PDI) = 1.43 (gel permeation chromatography, GPC)) was studied in *n*-hexane, a PDMS block selective solvent. Transmission electron microscopy (TEM), atomic force microscopy (AFM), and TEM with negative staining analysis of these micellar solutions after solvent evaporation revealed the presence of multiple micellar morphologies including spheres, cylinders, and novel flower-like supramolecular aggregates. TEM analysis of samples fractionated by ultracentrifugation and preparative size-exclusion chromatography suggest that the formation of multiple morphologies is a consequence of compositional variations. When micellar solutions were prepared at 50 °C (above the glass transition of the PFDMS core-forming block) flower-like micellar aggregates similar to those present in micellar solutions prepared at room temperature also formed. However, after solvent evaporation, TEM analysis of micellar solutions prepared in decane at about 150 °C, above the melt temperature of the PFDMS core (ca. 120 – 145 °C), revealed the presence of spherical micelles (when decane solutions at 150 °C were rapidly cooled to room temperature) and rod-like cylindrical micelles (when decane solutions at 150 °C were slowly cooled to room temperature). In contrast, poly(ferrocenylmethylethylsilane)-*block*-poly(dimethylsiloxane)-*block*-poly(ferrocenylmethylethylsilane) (PFMES-*b*-PDMS-*b*-PFMES, **4**; block ratio 1:16:1; $M_n = 2.90 \times 10^4$ g mol^{-1}, PDI = 1.42 (GPC)) and poly(ferrocenylmethylphenylsilane)-*block*-poly(dimethylsiloxane)-*block*-poly(ferrocenylmethylphenylsilane) (PFMPS-*b*-PDMS-*b*-PFMPS, **5**; block ratio 1:15:1; $M_n = 3.00 \times 10^4$ g mol^{-1}, PDI = 1.38 (GPC)), which possess completely amorphous organometallic core-forming blocks, formed only spherical micelles in hexane at room temperature. These observations indicate that crystallinity of the insoluble polyferrocenylsilane block is a critical factor in the formation of the nonspherical micelle morphologies.

Keywords: micelles · nanostructures · organometallic polymers · polyferrocene · self-assembly · triblock copolymers

Introduction

The aggregation of amphiphilic block copolymers in block selective solvents to yield well-defined micellar structures is of considerable current interest. Typically, such aggregates are spherical with a dense core comprising the insoluble block surrounded by a solvent swollen corona of the soluble block.[1, 2] Until recently, the observation of nonspherical morphologies has been rare, and even now our understanding of them remains limited.[3, 4]

[a] Prof. I. Manners, Prof. M. A. Winnik, Dr. R. Resendes, Dr. J. A. Massey, K. Temple, L. Cao, K. N. Power-Billard
Department of Chemistry, University of Toronto
80 St. George Street, Toronto, Ontario, M5S 3H6 (Canada)
Fax: (+1) 416-978-6157
E-mail: imanners@alchemy.chem.utoronto.ca
mwinnik@alchemy.chem.utoronto.ca

The most well-studied class of block copolymer amphiphiles are the AB diblock copolymers. Materials of this type are typically synthesized through the use of sequential, living anionic polymerization routes as this affords well-defined block copolymers with narrow molecular weight distributions.[5] The self-assembly of the resulting polymers provides an attractive and potentially powerful route to nanostructured materials as illustrated by recent studies of block copolymer films and solution micelles containing metal or semiconductor nanoparticles in desired domains.[6]

Compared to the effort directed at understanding the self-assembly of amphiphilic AB block copolymers, amphiphilic triblock copolymers are much less studied. The triblock materials, poly(ethylene oxide)-*block*-poly(propylene oxide)-*block*-poly(ethylene oxide) (PEO-*b*-PPO-*b*-PEO, known commercially as *Pluronics*) are perhaps the most well-investigated triblock copolymer amphiphiles and currently find

0947-6539/01/0711-2414 $ 17.50+.50/0 *Chem. Eur. J.* **2001**, *7*, No. 11

uses in a variety of biomedical applications.[7] In a similar manner to AB diblock copolymers, ABA and ABC triblock copolymers generally self-assemble into well-defined spherical micelles in the presence of block-selective solvents, whereas nonspherical morphologies are rare.[8, 9] Triblock copolymers of the type ABA can also be viewed as telechelic homopolymers. Theoretically, in a specific solvent for the B block, at low concentrations self-assembly into two different types of spherical micelles can occur (Figure 1). In type **A** (open flower) spherical micelles only one of the insoluble blocks participates in the micelle core, while the other block remains in solution. In type **B** (closed flower) spherical micelles both of the insoluble blocks participate in the micelle core at the entropic expense of the folded soluble block. Which type of spherical micelle forms depends on the strength of the interaction between the solvent and core-forming block and the flexibility of the soluble block (a highly flexible soluble block would allow the formation of type **B** micelles).[10–13] Importantly, type **A** spherical micelles could potentially allow intermicellar core cross-linking to occur by acting as tie molecules; this could lead to the formation of interesting supramolecular aggregates.

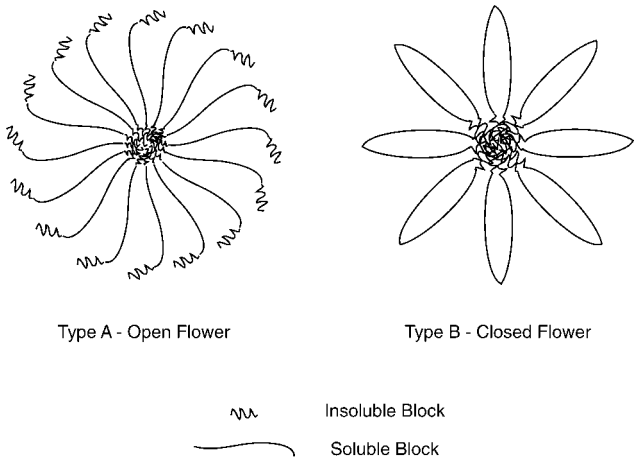

Figure 1. Schematic representations of the two extreme scenarios for spherical micelles derived from ABA triblock copolymers. a) In type **A** micelles, only one of the core forming blocks of a triblock copolymer chain participates in the micellar core. b) In type **B** micelles, both of the core forming blocks are present in the micellar core.

Recently there has been a significant effort aimed at the incorporation of electroactive polymer segments into amphiphilic block copolymer architectures. Within the realm of triblock copolymers, recent studies focussing on the incorporation of polythiophene, poly(*p*-phenylene vinylene), and polysilane blocks into triblock copolymers have been reported.[14–16] In addition, Schmidt and co-workers have recently synthesized an ABC triblock copolymer, with a hole-transporting, a chromophore-containing, and an electron-transporting block; this polymer functions as an electroluminescent material.[17]

The discovery that strained silicon-bridged [1]ferrocenophanes undergo living anionic ring-opening polymerization (ROP) has made possible the synthesis of well-defined amphiphilic block copolymers that incorporate polyferrocene blocks.[18, 19] As part of our work in this area, we have recently reported studies of the self-assembly of poly(ferrocenyldimethylsilane)-*block*-poly(dimethylsiloxane) (PFDMS-*b*-PDMS, **1**; PFDMS:PDMS block ratio of 1:6, $M_n = 3.75 \times 10^4\ g\,mol^{-1}$, PDI = 1.10) in the solid state and in solution. Thin films of this material self-assemble to form a hexagonal array of PFDMS cylinders within a PDMS matrix, whereas in *n*-hexane, a solvent selective for the PDMS block, cylindrical micelles are formed with a core of PFDMS surrounded by a sheath of solvent swollen PDMS.[20, 21] Phase separation results in highly metal-rich nanodomains; since the redox active PFDMS homopolymer becomes semiconducting on oxidative doping and functions as a precursor to magnetic ceramics, these structures represent intriguing prospective precursors to semiconducting or magnetic nanowires.[22–25]

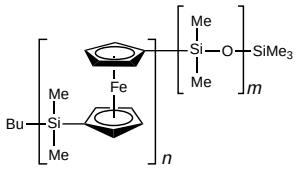

PFDMS-*b*-PDMS

1

In light of the interesting potential applications of polyferrocene block copolymers, it would be desirable to find a less experimentally demanding route to these materials. In 1998, we reported the synthesis of polyferrocene multiblock copolymer architectures through a facile transition-metal-catalyzed ROP approach in which polyferrocene blocks are "grown" from terminal Si–H functionalities.[26, 27] This very convenient methodology simply requires the addition of the [1]ferrocenophane monomer, **2** (R = R′ = Me), to commercially available Si–H end-functionalized poly(dimethylsiloxane) in the presence of a Pt^0 (Karstedt's) catalyst (Scheme 1).

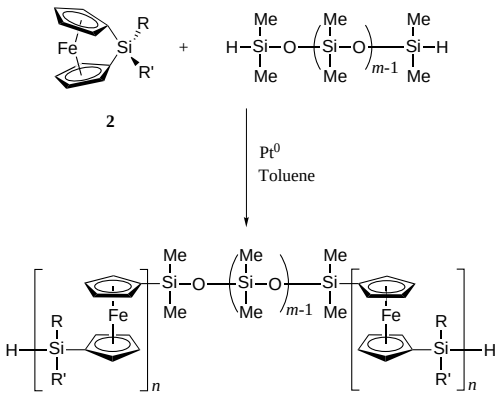

3a: *n* = 11, *m* = 81; R = R' = Me
3b: *n* = 21, *m* = 270; R = R' = Me

Scheme 1. Synthesis of polymers **3a** and **3b**.

Recently, we described preliminary studies of the solution self-assembly of an amphiphilic PFDMS-*b*-PDMS-*b*-PFDMS triblock polymer, **3b**, prepared by this route.[28] In this paper, we now report full details on the solution self-assembly of **3b**, and our studies aimed at understanding the factors which govern this process.

Results and Discussion

Synthesis and structural characterization of PFDMS-*b*-PDMS-*b*-PFDMS triblock copolymers 3a and 3b: The PFDMS-*b*-PDMS-*b*-PFDMS block copolymers **3a** and **3b** were prepared through the transition-metal-catalyzed ROP of **2** (R = R′ = Me) in the presence of Si–H end-functionalized PDMS. A low molecular weight PFDMS-*b*-PDMS-*b*-PFDMS block copolymer, **3a**, was initially prepared as a model to confirm the triblock structure. Polymer **3a** was isolated as an orange powder and ^{1}H and ^{29}Si NMR spectroscopy confirmed the proposed structure. The ^{1}H NMR spectrum of **3a** (in C_6D_6) revealed two broad resonances centered at $\delta = 4.26$ and 4.09, attributable to the α and β protons of the Cp rings, as well as singlet resonances at $\delta = 0.54$ and 0.28 due to the Me groups of the PFDMS and PDMS blocks, respectively. ^{1}H NMR integration indicated that **3a** possessed a PFDMS:PDMS:PFDMS block ratio of approximately 1:7:1 and gel permeation chromatographic (GPC) analysis of this material revealed a molecular weight of $M_n = 8.14 \times 10^3$ g mol^{-1} with a polydispersity (PDI) of 1.45. Of note in the ^{29}Si NMR of **3a** are the singlet resonances at $\delta = -6.4$ and -21.4 that correspond to the interior silicon environments of the PFDMS and PDMS blocks, respectively. Additionally, singlet resonances were also observed at $\delta = 0.7$ and -18.2 that correspond to the Me_2SiO–fc (fc = ferrocene) switching groups and the fc–$SiMe_2H$ end groups of polymer **3a**, respectively (Figure 2). These observations, in addition to the absence of a ^{1}H NMR resonance at $\delta = 4.95$ and a ^{29}Si NMR resonance δ at $= -6.50$ (Figure 2 inset), attributable to the $-OSiMe_2H$ end group of the initial PDMS telechelic, confirmed the ABA triblock structure of polymer **3a** as that depicted in Scheme 1. Contamination by PFDMS homopolymer was not detected as the molecular weight of this material when formed by Pt-catalyzed ROP in the absence of a Si–H-capping reagent is 10^5–10^6, and a bimodal molecular weight distribution would be anticipated which was not observed. As the Si–H bonds of the PDMS telechelic are expected to be very reactive, a triblock product would be expected. Although contamination by AB diblock was below the NMR detection limit, the presence of small amounts of this material cannot be ruled out.

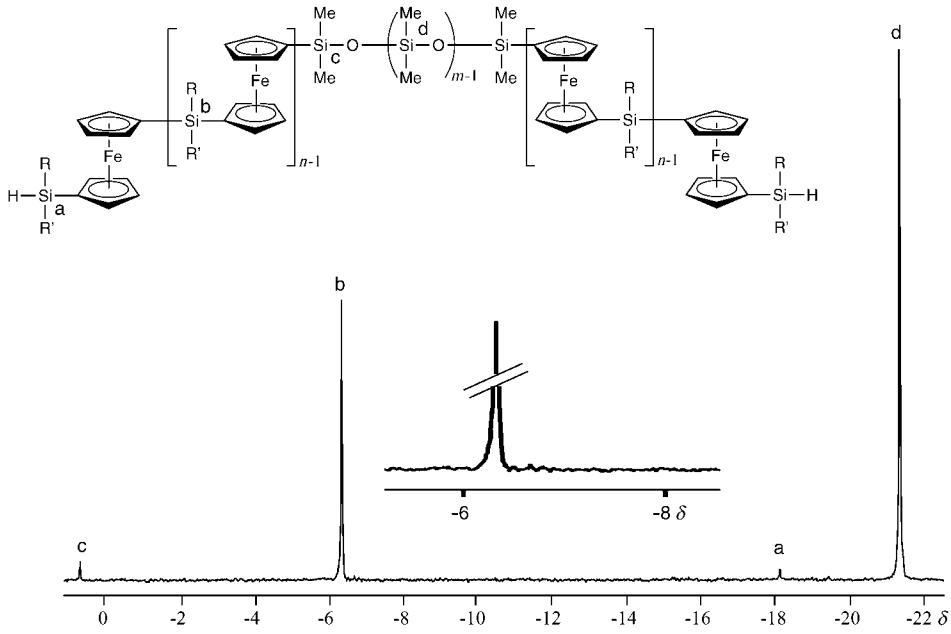

Figure 2. ^{29}Si NMR spectrum (C_6D_6) of **3a** revealing switching groups between the PFDMS and PDMS blocks.

In an effort to obtain a PFDMS-*b*-PDMS-*b*-PFDMS triblock copolymer that would self-assemble in a PDMS block-selective solvent, a higher molecular weight triblock copolymer (**3b**) with greater PDMS content was prepared (Scheme 1). Polymer **3b** was isolated as an orange gum after precipitation of the crude reaction mixture into methanol. ^{1}H and ^{29}Si NMR (in C_6D_6) analysis of polymer **3b** confirmed the ABA triblock structure to be analogous to that depicted in Scheme 1. ^{1}H NMR integration indicated a PFDMS:PDMS:PFDMS block ratio of 1:13:1, and GPC analysis revealed a molecular weight of $M_n = 2.88 \times 10^4$ g mol^{-1} with a PDI of 1.43. The ^{29}Si NMR spectrum of **3b** revealed two singlet resonances at $\delta = -6.4$ and -21.4, which correspond to the interior silicon environments of the PFDMS and PDMS blocks of **3b**, respectively. No end groups or switching groups, like those observed for polymer **3a**, were apparent in the ^{29}Si NMR of polymer **3b**; this is expected owing to the substantially higher molecular weight, hence, the lower concentration of end groups and switching groups, possessed by this material (cf. **3a**). Differential scanning calorimetry (DSC) analysis revealed thermal transitions close to those of the constituent homopolymers, consistent with phase separation in the solid state. Specifically, the glass transition temperatures (T_g) and melting temperatures (T_m) for both the PFDMS ($T_g = 26\,^\circ$C, $T_m = 130\,^\circ$C) and PDMS ($T_g = -123\,^\circ$C, $T_m = -44\,^\circ$C) blocks were observed in addition to the crystallization ($T_{cryst} = -103\,^\circ$C) of the PDMS block (Figure 3). In addition, wide-angle X-ray scattering (WAXS) experiments revealed that the triblock copolymer in the bulk was semicrystalline, with peaks consistent with those observed for bulk PFDMS.[29]

Solution aggregation of PFDMS-*b*-PDMS-*b*-PFDMS triblock copolymers 3a and 3b: Although the observed molecular weight distributions for **3a** and **3b** obtained through this transition-metal-catalyzed ROP methodology are broader than those typically observed through living anionic polymer-

0947-6539/01/0711-2416 $ 17.50+.50/0 *Chem. Eur. J.* **2001**, *7*, No. 11

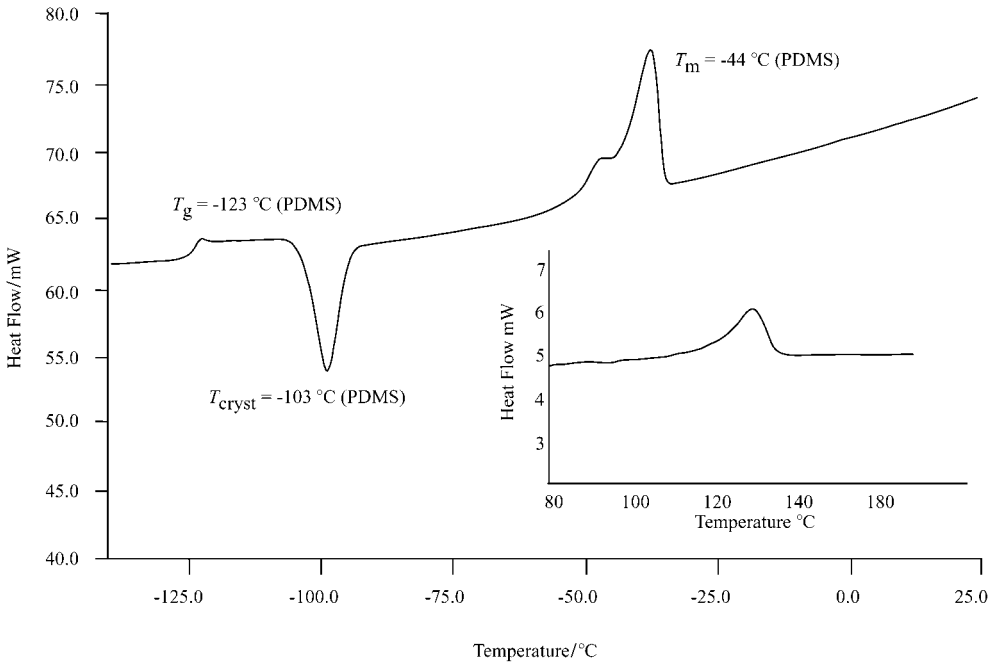

Figure 3. Differential scanning calorimetry (DSC) thermogram of **3b**. The T_m for the PFDMS block is shown in the inset (obtained in a separate experiment). The T_g (26 °C) is present, but not shown.

ization routes (PDI typically >1.3 compared with <1.3) we were particularly encouraged by recent studies of an amphiphilic polysilane/PEO-alternating multiblock copolymer ($M_n = 2.7 \times 10^4$ g mol^{-1}). This demonstrated that despite a fairly broad molecular weight distribution (PDI = 1.6) well-defined supramolecular vesicular aggregates were formed in water.[30]

We were unable to prepare solutions of **3a** in *n*-hexane. This observation is consistent with the lower PDMS content present in polymer **3a** when compared with that present in polymer **3b**. In contrast, polymer **3b** forms micellar solutions in *n*-hexane, a good solvent for PDMS and a precipitant for PFDMS. A micellar solution was prepared by first dissolving **3b** in THF, a good solvent for both blocks, and subsequently adding *n*-hexane slowly until the resulting solution became turbid. The onset of solution turbidity was taken as an indication of micelle formation. The resulting solution was then dialyzed against pure *n*-hexane to remove the THF. Dynamic light scattering (DLS) analysis of the resulting micellar solutions revealed the presence of large aggregates (>3 μm) in solution. TEM analysis of these aggregates after solvent evaporation revealed three main, co-existent morphologies. Specifically, **3b** was found to assemble into spherical micelles, cylindrical micelles, and novel, flower-like aggregates (Figure 4).[31] Careful examination of Figure 4 suggests that these flower-like structures (which are to be distinguished from the flower-like micelles in Figure 1) are in fact supramolecular aggregates of individual cylindrical micelles. These superstructures are approximately 3–5 μm in diameter, consistent with DLS data, and each individual micellar "arm" is approximately 15–17 nm in diameter. The average diameter of the individual cylindrical micelles is in good agreement with that observed by TEM for the cylindrical micelles found in micellar solutions of amphiphilic diblock copolymer **1** (ca. 20 nm).[20, 21] As TEM relies on contrast provided by electron-density differences, this technique allowed the selective imaging of the iron-containing PFDMS cores. Analysis of the dialyzed *n*-hexane solution of **3b** by atomic force microscopy (AFM) allowed both the PFDMS core and the PDMS corona to be visualized, and showed the presence of supramolecular flower-like aggregates consistent in size and shape with the flower-like cores imaged by TEM (Figure 5). Interestingly, the average diameter of the individual cylindrical micelles was found to be approximately 70 nm, that is, about 55 nm greater than that observed by TEM. This observation is consistent with the fact that AFM

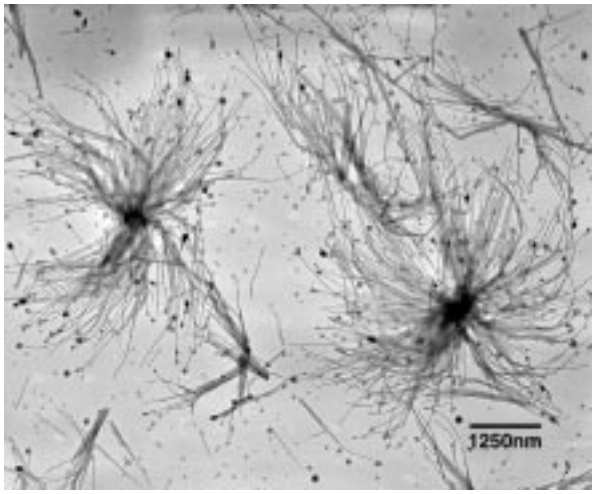

Figure 4. TEM micrograph obtained by aerosol spraying a dilute, dialyzed solution of **3b** from *n*-hexane onto a thin carbon film supported on mica. It was not necessary to stain the sample as the iron-rich domains provided sufficient contrast. The micrograph revealed three distinct and coexistent micellar morphologies.

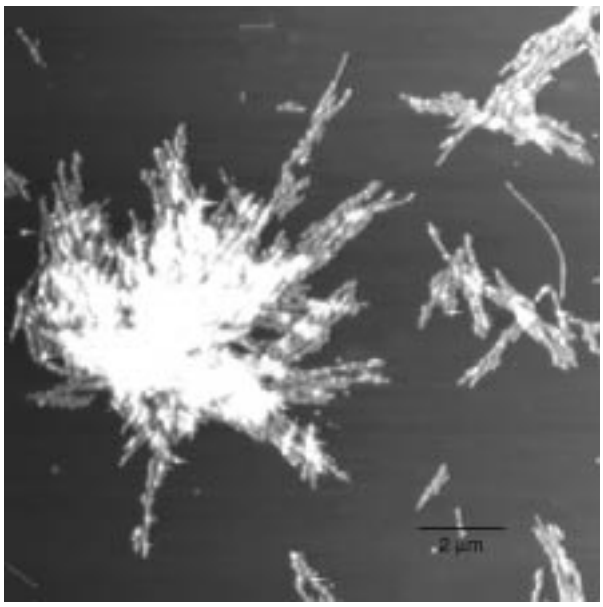

Figure 5. AFM micrograph (phase image) of flower-like micelles of **3b** (from a dialyzed solution in *n*-hexane).

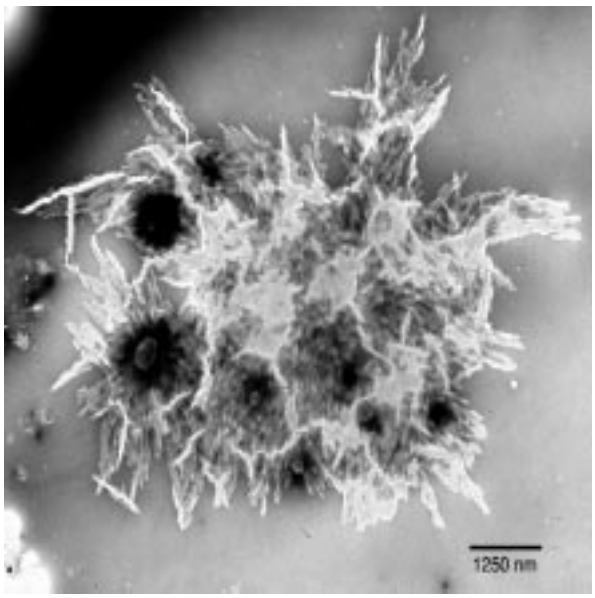

Figure 6. TEM micrograph of micellar solution of **3b**, after solvent evaporation, obtained from NSTEM. Unlike normal TEM experiments, which only image the electron-rich PFDMS cores, the NSTEM experiment images the entire micellar morphology.

measurements image the whole of the micellar assembly as opposed to only the iron-rich PFDMS cores imaged by TEM.

In order to further investigate the structures of the supramolecular aggregates imaged by TEM and AFM, a negative stain TEM (NSTEM) experiment was undertaken. In NSTEM, the sample and substrate are treated with dodecatungstophosphoric acid ($H_3PO_4 \cdot 12\,WO_3 \cdot x\,H_2O$); this results in the substrate (i.e., the carbon film) becoming selectively stained, while leaving the micellar aggregates unaltered.[32] In such a measurement, the whole of the micellar assembly is imaged, unlike in normal TEM samples in which only the iron-rich PFDMS cores are visualized. Therefore, like AFM, NSTEM images the whole of the micellar assembly. Hence, when NSTEM analysis of micellar solutions of **3b** was undertaken, supramolecular flower-like aggregates with particle diameters of approximately 3–5 μm were observed (Figure 6), consistent with those seen by TEM and AFM. Interestingly, the average diameter of the individual cylindrical micelles making up the supramolecular aggregates, was found to be about 63 nm. This value is not as high as determined by AFM (ca. 70 nm) and is consistent with the broadening of micellar dimensions in AFM images known to occur due to tip deconvolution effects.[33]

Composition and molecular weight dependence on the observed micellar morphology of 3b: The relatively large PDI value of polymer **3b** (PDI = 1.43) introduces a significant amount of compositional variation. In order to investigate the influence of this variable on the observed morphology, fractionation was performed. Centrifugation (1.5×10^4 rpm for 20 min) of the dialyzed *n*-hexane solution of **3b** resulted in the formation of a two-phase system with a very light, amber supernatant solution and a yellow precipitate. Preliminary TEM analysis of the supernatant, after solvent evaporation, showed it to be composed almost entirely of spherical micelles. However, subsequent TEM studies of this fraction revealed that in fact two separate morphologies were present, namely spherical micelles which were approximately 20–40 nm in diameter in addition to significantly larger (ca. 100–150 nm) compound micelles (Figure 7 top). ^{1}H NMR integration of this fraction gave an approximate PFDMS:PDMS:PFDMS block ratio of 1:60:1, indicative of a much smaller PFDMS content relative to the unfractionated sample; GPC analysis (in THF) revealed this fraction to be of lower molecular weight ($M_n = 2.52 \times 10^4$ g mol^{-1}, PDI = 1.50).

The yellow precipitate obtained by centrifugation could be redispersed in hexane. TEM analysis after solvent evaporation showed the presence of flower-like aggregates and short cylindrical micelles (Figure 7 bottom). ^{1}H NMR integration of this sample revealed a PFDMS:PDMS:PFDMS block ratio of approximately 1:6:1 consistent with a significantly larger PFDMS content relative to that found for the unfractionated sample. GPC analysis of this fraction revealed a higher molecular weight ($M_n = 3.97 \times 10^4$ g mol^{-1}, PDI = 1.37) relative to that found for unfractionated **3b**. These initial observations suggest that, in contrast to the polysilane-*b*-PEO multiblock system mentioned above, the variation in the block ratios present in unfractionated **3b** plays a key role in the formation of multiple micellar morphologies. Thus, the component with short PFDMS blocks appear to give rise to the spherical structures, whereas longer PFDMS blocks allow cylinders and flower-like aggregates to be formed.

In order to investigate how the morphology varies with molecular weight a sample of **3b** was fractionated by preparative size-exclusion chromatography in THF, and three fractions were isolated (Table 1) The three isolated fractions had mean molecular weights and polydispersities of $M_n = 2.60 \times 10^4$ g mol^{-1}, PDI = 1.31; $M_n = 3.88 \times 10^4$ g mol^{-1}, PDI = 1.23; and $M_n = 6.10 \times 10^4$ g mol^{-1}, PDI = 1.18 (Figure 8). The PDI values were significantly smaller than for the unfractionated polymer (PDI = 1.43). Interestingly,

  0947-6539/01/0711-2418 $ 17.50+.50/0

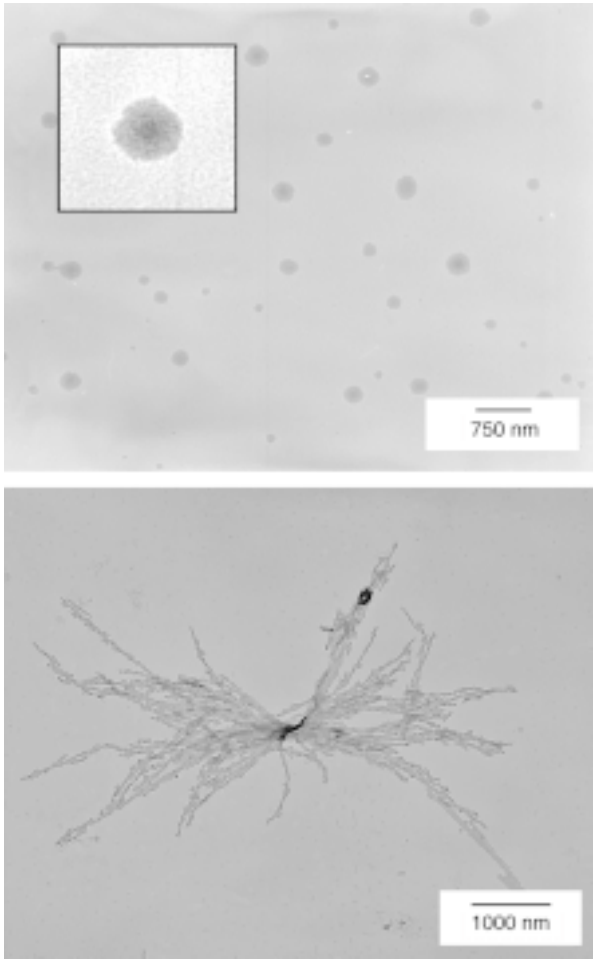

Figure 7. TEM micrograph of spherical and compound (see inset) micelles present in the supernatant (top) and redissolved precipitate (bottom) obtained from the fractionation of **3b**.

Table 1. Summary of molecular weights and relative compositions obtained for **3b** through preparative size exclusion chromatography.

Fraction	M_n ($\times 10^4$)	PDI	PFDMS:PDMS:PFDMS[a]
1	6.10	1.18	1:14:1
2	3.88	1.23	1:14:1
3	2.60	1.31	1:14:1

[a] Determined by ^{1}H NMR spectroscopy.

^{1}H NMR analysis of these fractions revealed that despite the significant differences in molecular weights, the overall composition (PFDMS:PDMS:PFDMS) of each fraction was 1:14:1 (cf. unfractionated **3b**, where PFDMS:PDMS:PFDMS = 1:13:1; see Table 1). When *n*-hexane solutions of fractions 1–3 were studied by TEM, after aerosol spraying, similar flower-like aggregates to those observed for *n*-hexane solutions of unfractionated **3b** were observed. Given that the molecular weights of each fraction were quite different and that the overall compositions measured in each case were very similar to that for unfractionated **3b**, the observation of flower-like aggregates from *n*-hexane solutions of fractions 1–3 suggests that for the molecular weights studied, the overall block ratio and not the molecular weight influences the observed micellar morphology.

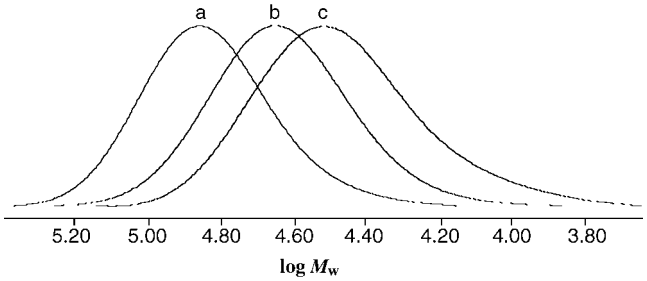

Figure 8. GPC traces of **3b** fractionated with preparative size exclusion column. a) $M_n = 6.10 \times 10^4$ g mol^{-1}, PDI = 1.18; b) $M_n = 3.88 \times 10^4$ g mol^{-1}, PDI = 1.23; and c) $M_n = 2.60 \times 10^4$ g mol^{-1}, PDI = 1.31.

Micellization behavior of 3b above the T_g of the PFDMS block: In the experiments reported to this point the micellization was performed at room temperature (22 °C). The T_g of the PFDMS homopolymer is 33 °C[24] and, as noted earlier, the T_g of the PFDMS block in **3b** is 26 °C. As the micellization is taking place below the T_g of the PFDMS block, it is possible that the observed flower-like aggregates are kinetic structures that form as a consequence of the glassy micellar cores.

In order to explore the possible dependence of the observed micellar morphologies on whether micellization is performed below or above the T_g of the PFDMS block, self-assembly of **3b** in hexane was performed at 50 °C. In addition, samples were prepared at three different concentrations (initially 50 mg mL^{-1}, 100 mg mL^{-1}, and 250 mg mL^{-1} in THF) in order to investigate any concentration dependence. When the micellar solutions of **3b** prepared at 50 °C were examined by TEM after solvent evaporation, flower-like aggregates similar to those seen for *n*-hexane solutions of **3b** prepared at room temperature were observed at every concentration. This observation suggests that whether micellization is performed below or above the glass transition temperature of the PFDMS core-forming block does not play a significant role determining the micellar morphologies formed.

Micellization behavior of 3b above the T_m of the PFDMS block—evidence for the influence of crystallinity of the polyferrocenylsilane block on the observed micellar morphologies: Previous work has shown that PFDMS homopolymers will crystallize at $T_m = 120–145$ °C.[24,29] Earlier in this paper we reported evidence from DSC and WAXS analysis that the PFDMS blocks also crystallize in bulk samples of **3b**. In order to investigate the influence of the crystallinity of the PFDMS block on the micellar morphology, micellar solutions (6.6 mg mL^{-1}) were prepared by heating samples of **3b** in decane (a PDMS selective solvent) above the T_m of the PFDMS block. First, for comparison purposes, decane solutions of **3b** were prepared at room temperature by dissolving **3b** in THF (100 mg mL^{-1}) and slowly adding decane until micellization had occurred. When these samples were investigated by TEM, similar flower-like aggregates to those formed in *n*-hexane were observed. Samples were then prepared by heating **3b** in decane at 150 °C for 1 h followed by rapid cooling in an ice bath. Analysis by TEM after aerosol-spraying the solution onto carbon films showed the presence of only spherical micelles which were approximately 40–60 nm in diameter (Figure 9 top). No flower-like assem-

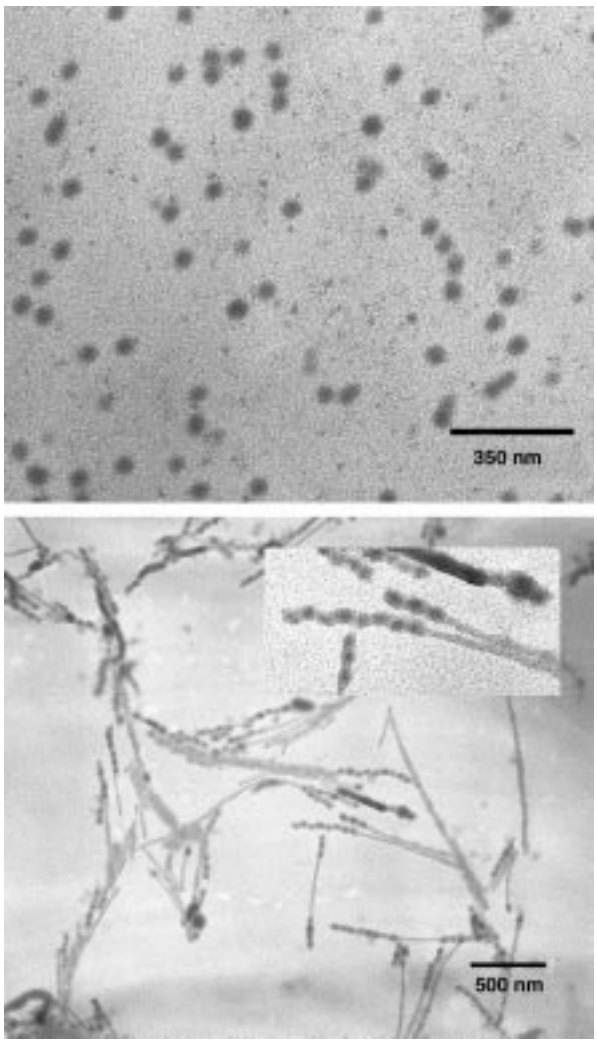

Figure 9. TEM micrographs of micellar solutions of **3b**, after solvent evaporation, prepared in decane at 150 °C followed by rapid cooling to room temperature (top) and slow cooling to room temperature (bottom).

blies were observed in any of the samples studied. Interestingly, when the micellar solutions of **3b** prepared in decane at 150 °C for 1 h were allowed to cool to room temperature slowly (over a period of ca. 2 h), TEM analysis showed the presence of cylindrical micelles which were about 15–20 nm in diameter. These are similar in dimension to the individual cylindrical micelles found in the flower-like aggregates (Figure 9 bottom). Moreover, some segments of the cylindrical micelles were found to be comprised of individual spherical micelles which have presumably linked together to give a "pearl necklace" type of morphology (see Figure 9 bottom, inset). Since the micellar solutions prepared at 150 °C were at temperatures significantly higher than the T_m of the PFDMS block, the observation of spherical micelles on rapid cooling and cylindrical micelles on slow cooling suggests that crystallization of the PFDMS block may be critical to the assembly of **3b** into flower-like superstructures.

We note that the spherical aggregates present in micellar solutions of **3b** prepared in decane at 150 °C followed by rapid cooling are significantly larger (ca. 40–60 nm in diameter) than the spherical micelles present in micellar solutions (in *n*-hexane, prepared at 25 °C) obtained from fractionated samples of **3b** (PFDMS:PDMS:PFDMS block ratio of 1:60:1, $M_n = 2.52 \times 10^4$ g mol^{-1}, PDI = 1.50) which were approximately 20–40 nm in diameter. This observation is consistent with the fact that the PFDMS content of fractionated **3b** is significantly lower than that found in unfractionated **3b** (PFDMS:PDMS:PFDMS block ratio of 1:13:1, $M_n = 2.88 \times 10^4$ g mol^{-1}, PDI = 1.43). The average diameter is also greater than that of the cylinders formed on slow cooling (15–20 nm, Figure 9, bottom). We have no detailed explanation for this observation as yet, but we feel that it underlines how kinetic factors are critical to the determination of the micellar size and structure in this triblock system.

In order to further understand these phenomena, two additional ABA triblock copolymers, poly(ferrocenylmethylethylsilane)-*block*-poly(dimethylsiloxane)-*block*-poly(ferrocenylmethylethylsilane) (PFMES-*b*-PDMS-*b*-PFMES, **4**) and

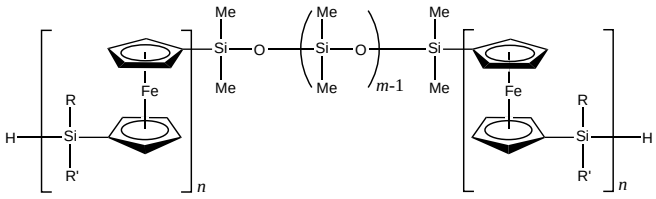

4: *n* = 17, *m* = 270; R = Me, R' = Et
5: *n* = 18, *m* = 270; R = Me, R' = Ph

poly(ferrocenylmethylphenylsilane)-*block*-poly(dimethylsiloxane)-*block*-poly(ferrocenylmethylphenylsilane) (PFMPS-*b*-PDMS-*b*-PFMPS, **5**) were prepared. Triblock copolymers **4** and **5** possess completely amorphous PFMES ($T_g = 15$ °C)[34] and PFMPS ($T_g = 90$ °C)[24] core-forming blocks, respectively, and were expected to provide further insight into the influence of crystallinity on the observed micellar morphology.

Synthesis and solution self-assembly of PFMES-*b*-PDMS-*b*-PFMES and PFMPS-*b*-PDMS-*b*-PFMPS triblock copolymers 4 and 5: Triblock copolymers **4** and **5** were synthesized by employing the same transition-metal-catalyzed methodology used in the synthesis of copolymers **3a** and **3b**. Specifically, ROP of **2** (R = Me, R′ = Et) and **2** (R = Me, R′ = Ph) in the presence of Si–H end-functionalized PDMS resulted in the isolation of triblock copolymers **4** ($M_n = 2.90 \times 10^4$ g mol^{-1}, PDI = 1.42) and **5** ($M_n = 3.00 \times 10^4$ g mol^{-1}, PDI = 1.38), respectively. ^{1}H and ^{29}Si NMR (in C_6D_6) analysis of polymers **4** and **5** confirmed the ABA triblock structure and ^{1}H NMR integration revealed copolymers **4** and **5** to possess polyferrocene:PDMS:polyferrocene block ratios of 1:16:1 and 1:15:1, respectively. Due to the presence of different substituents on the silicon centers of the polyferrocene blocks, the ^{1}H NMR spectra of both **4** and **5** exhibit four unique Cp resonances. The ^{29}Si NMR spectra for polymers **4** and **5** show resonances for the interior Si environments of the PFMES ($\delta = -4.3$) and PFMPS ($\delta = -11.3$) blocks as well as resonances for the interior Si environments of the PDMS blocks (for **4**: $\delta = -21.8$, for **5**: $\delta = -21.9$). As the molecular weights

0947-6539/01/0711-2420 $ 17.50+.50/0 *Chem. Eur. J.* **2001**, *7*, No. 11

of polymers **4** and **5** were quite high, ^{29}Si NMR resonances due to end groups or switching groups could not be detected.

Micellar solutions of **4** and **5** were prepared by first dissolving samples of polymers **4** or **5** in THF (a good solvent for both the PFMES/PFMPS and PDMS blocks) followed by the slow addition of *n*-hexane until the onset of turbidity. Dialysis of these micellar solutions against pure *n*-hexane removed the remaining THF. TEM analysis of the contents of the micellar solutions of **4**, after solvent evaporation, revealed the presence of spherical micelles which were found to possess average core diameters ranging from 20–30 nm (Figure 10 top). In all subsequent TEM measurements, only spherical micelles were observed with no evidence for the formation of flower-like superstructures.

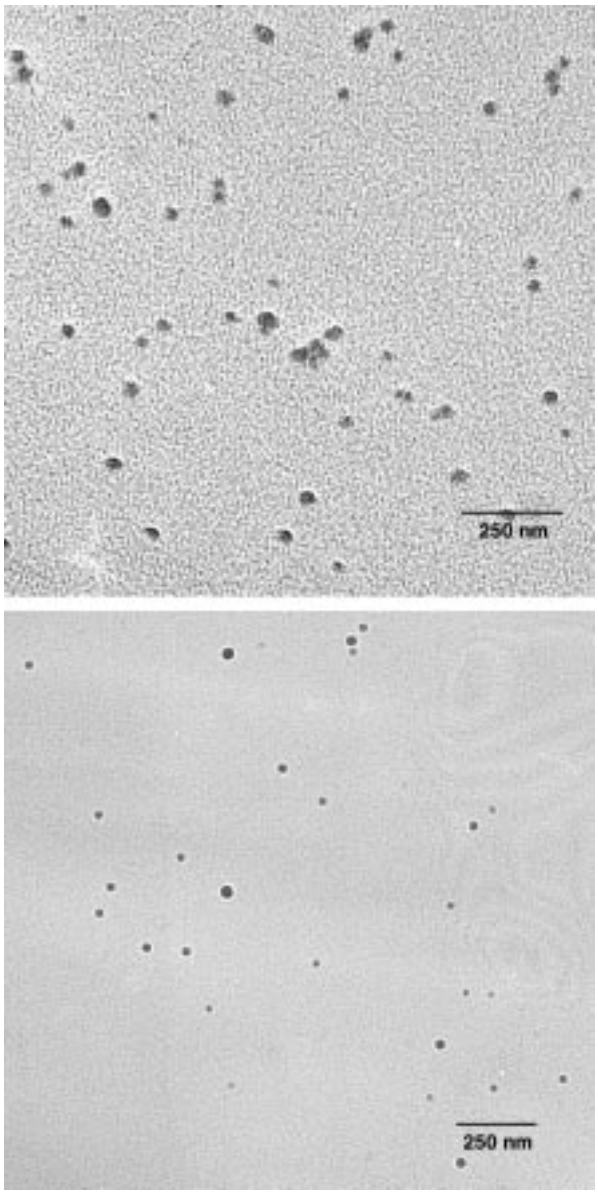

Figure 10. TEM micrographs of micellar solutions of **4** (top) and **5** (bottom) in *n*-hexane, after solvent evaporation.

TEM analysis of micellar solutions of **5** after solvent evaporation also revealed the presence of spherical micelles (Figure 10 bottom). As for the case of **4**, no cylindrical micelles or any higher order supramolecular aggregates were observed. The spherical micelles of **5** possess average core diameters ranging from 20–30 nm, which are similar to those observed for **4**.

These observations lend further support to the concept that crystallization of the PFDMS block plays a key role in the morphologies formed in the solution self-assembly of **3b**.

WAXS analysis of micelles and superstructures from 3b—evidence for crystallization of PFDMS blocks: The results of our studies of the solution self-assembly of **3b**, **4**, and **5** suggest that crystallization of the PFDMS block plays a key role in the formation of the multiple morphologies and superstructures from **3b**. In order to confirm the presence of crystallinity in the latter, micellar aggregates were prepared in *n*-hexane at room temperature and were analyzed by WAXS after solvent evaporation. The WAXS pattern (Figure 11) showed discrete reflections at 7.41 Å and 6.58 Å similar to those present in bulk samples of **3b**.[29]

This result indicates that significant crystallinity is indeed present in the micelles and superstructures formed by the self-assembly of **3b**.

Morphology evolution with time—crystallization directed self-assembly: An intriguing question is: How do the flower-like superstructures form? The cylindrical micelles of **3b** prepared in decane at 150 °C followed by slow cooling to 25 °C possessed diameters ranging from 15–20 nm, similar to those for the individual micellar "arms" of the flower-like aggregates obtained from **3b** below the T_m of the PFDMS block. Furthermore, the observation of "pearl necklace"/cylindrical micelle hybrid structures (Figure 9 bottom, inset) suggest that the cylindrical micelles observed in micellar solutions of **3b** prepared in decane at 150 °C followed by slow cooling may be the result of a slow transition from spherical to cylindrical micelles.

To provide further insight, we carried out preliminary investigations of the time evolution of the morphology of **3b** in hexane at ambient temperatures. When **3b** was self-assembled in hexane and the resulting aggregates immediately analyzed by TEM only spherical micelles of diameter 40–70 nm were observed. Subsequent TEM analysis after 2 min showed the presence of flower-like assemblies similar to those discussed previously. Although clearly further detailed studies are needed, these observations tentatively suggest that the formation of flower-like supramolecular assemblies is a multistage process and that these superstructures evolve from spherical micelles.

Another very interesting question that remains is: How does the PFDMS crystallization direct micellization and superstructure formation? This is a complex issue and at this stage our explanation is limited. However, we note that the WAXS pattern for the flower-like aggregates (Figure 11) is similar to that for the PFDMS homopolymer[29] and is analogous to that for single crystals of the corresponding linear pentamer.[35] Based on the structure of the latter, crystallization should lead to a preferred parallel arrangement of the PFDMS chains in the block copolymer; this in turn

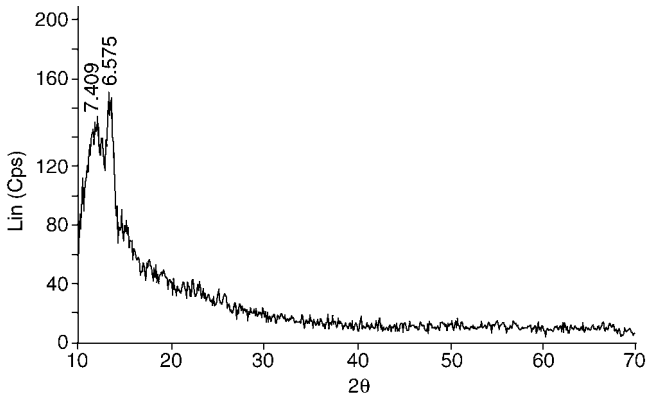

Figure 11. WAXS pattern of a micellar solution of **3b** (in *n*-hexane) after solvent evaporation.

should favor the formation of structures with low curvature (e.g., cylinders versus spheres).[36] This is consistent with the appearance of the flower-like superstructures which suggests that cylindrical micelles are a major component. In addition, the ability of triblock copolymers to act as "tie" molecules between domains would be expected to play a key role in superstructure formation.

Finally, we return to the observation that the block copolymer composition also influences the observed morphology. Specifically fractionation of **3b** yielded a sample with longer PFDMS blocks, which also formed flower like superstructures, and another sample with very short PFDMS blocks which did not (see above). We believe in the latter case the PFDMS blocks are so short that either formation of crystallites of substantial size is impeded or that the preference for spherical structures caused by the dramatic block asymmetry is so strong that low curvature structures are not formed.

Conclusions

Studies of the self-assembly of a polyferrocene triblock copolymer, **3b**, obtained by a facile transition-metal-catalyzed ROP methodology, have illustrated the reproducible formation of multiple morphologies and, in particular, the formation of novel flower-like superstructures. The observation of coexisting multiple morphologies in diblock and triblock copolymer systems of narrow polydispersity has been previously reported,[3, 4] whereas, as mentioned above, recent work has provided examples of systems in which well-defined aggregates are formed despite significant polydispersities (PDI = 1.6).[30] In our particular case, fractionation experiments suggest that the compositional variations associated with the polydispersity of **3b** (PDI = 1.43) play a key role in the formation of multiple micellar morphologies. Preparation and subsequent TEM analysis of the aggregates present in micellar solutions of **3b** in *n*-hexane at 50 °C also revealed the presence of flower-like micellar aggregates suggesting that the glassy regions of the PFDMS core do not significantly influence the observed morphology. However, TEM analysis of micellar solutions prepared in decane at 150 °C, above the melt transition for the PFDMS block, showed no evidence for the formation of flower-like aggregates. This observation suggests that the ability of the PFDMS core-forming block to crystallize is critical in directing the formation of flower-like supramolecular aggregates. Furthermore, the study of the solution self-assembly of triblock copolymers **4** and **5**, which possess amorphous polyferrocene blocks, revealed only the presence of spherical micelles. This observation further suggests that crystallinity is an important factor governing the formation of nonspherical micelles from **3b**, and this concept is likely to be a result of broad significance to other block copolymer systems.[36]

Experimental Section

Equipment and materials: All reactions were carried out under an atmosphere of prepurified nitrogen by using either Schlenk techniques or an inert-atmosphere glovebox (MBraun). Hexanes and THF were dried over Na/benzophenone and distilled immediately prior to use. The silicon-bridged [1]ferrocenophane monomers were synthesized according to literature procedures.[24, 34] Karstedt's catalyst (a divinyltetramethyldisiloxaneplatinum(0) complex) was purchased from Gelest Chemical Co. as a 3% by weight solution in xylenes. All other chemicals were purchased from Aldrich unless otherwise noted. ^{1}H NMR (400 MHz), ^{13}C NMR (100.5 MHz), and ^{29}Si NMR (79.5 MHz) spectra were recorded on a Varian Unity 400 spectrometer. Molecular weights were estimated by gel permeation chromatography (GPC) by using a Waters Associates liquid chromatograph equipped with a Model 510 HPLC pump, a Model U6 K injector, Ultrastyragel columns with pore sizes of 10^3–10^5 Å, and a differential refractometer as the detector. A flow rate of 1.0 mL min^{-1} was used, and the eluent was a solution of 0.1% tetra-*n*-butylammonium bromide in THF. Polystyrene standards purchased from American Polymer Standards were used for calibration purposes. Transmission electron micrographs were obtained on a Hitachi Model 600 electron microscope. AFM images were obtained using a Nanoscope III microscope (Digital Instruments) in tapping mode with a silicon cantilever with a resonance frequency of 300–380 kHz. Dynamic light scattering experiments were carried out on a variable-angle light-scattering photometer from Brookhaven Instruments Corporation. A 5 mW vertically polarized He-Ne laser from Spectra Physics was the light source. The solution was filtered through a disposable 0.8 μm filter from Millipore into a glass scattering cell. WAXS diffraction analysis was obtained on a Siemens D5000 $\theta/2\theta$ diffractometer with a $Cu_{K\alpha}$ source operating at 50 KV, 35 mA in step scan mode. The second beam was monochromatized by a Kevex solid state detector.

Synthesis of triblock copolymer PFDMS-*b*-PDMS-*b*-PFDMS (3a): Karstedt's catalyst in xylenes (43 μL of a 0.3% by weight solution) was added to a solution of **2** (R = R′ = Me) (1.16 g, 4.79 mmol) and Si–H-terminated PDMS (1.44 g, 0.24 mmol, $M_w = 6.02 \times 10^3$ g mol^{-1}, PDI = 1.24) in toluene (20 mL). After stirring for 24 h, the deep orange solution was precipitated into methanol (150 mL). The orange precipitate was washed with methanol (3×100 mL) and dried under vacuum. Yield: 1.95 g (75%); GPC: $M_n = 8.14 \times 10^3$ g mol^{-1}, PDI = 1.45; ^{1}H NMR (400 MHz, C_6D_6): $\delta = 0.28$ (s, 21 H; SiO*Me*$_2$), 0.54 (s, 6 H; fcSi*Me*$_2$), 4.09 (m, 4 H; C$_5$*H*$_4$), 4.26 (m, 4 H; C$_5$*H*$_4$), 5.08 (br, 1 H; SiMe$_2$*H*); ^{29}Si{^{1}H} NMR (79.5 MHz, C_6D_6, DEPT $J = 51$ Hz): $\delta = -21.4$ (s, O*Si*Me$_2$), −18.2 (s, fc*Si*Me$_2$H), −6.4 (s, fc*Si*Me$_2$), 0.7 (s, Me$_2$*Si*O-fc).

Synthesis of triblock copolymer PFDMS-*b*-PDMS-*b*-PFDMS (3b): Karstedt's catalyst in xylenes (64 μL of a 0.3% by weight solution) was added to a solution of **2** (R = R′ = Me) (1.73 g, 7.14 mmol) and Si–H-terminated PDMS (5.0 g, 0.25 mmol, $M_w = 2.00 \times 10^4$ g mol^{-1}, PDI = 1.60) in toluene (40 mL). After stirring for 24 h, the deep orange solution was precipitated into methanol (250 mL). The adhesive orange gum was washed with methanol (3×200 mL) and dried under vacuum. Yield: 4.80 g (71%); GPC: $M_n = 2.88 \times 10^4$ g mol^{-1}, PDI = 1.43; ^{1}H NMR (400 MHz, C_6D_6): $\delta = 0.28$ (s, 39 H; SiO*Me*$_2$), 0.55 (s, 6 H; fcSi*Me*$_2$), 4.10 (m, 4 H; C$_5$*H*$_4$), 4.27 (m, 4 H; C$_5$*H*$_4$); ^{29}Si{^{1}H} NMR (79.5 MHz, C_6D_6, DEPT $J = 51$ Hz): $\delta = -21.4$ (s, O*Si*Me$_2$), −6.4 (s, fc*Si*Me$_2$).

Synthesis of triblock copolymer PFMES-*b*-PDMS-*b*-PFMES (4): Karstedt's catalyst in xylenes (37 μL of a 0.3% by weight solution) was added

0947-6539/01/0711-2422 $ 17.50+.50/0 *Chem. Eur. J.* **2001**, *7*, No. 11

to a solution of **2** (R = Me, R′ = Et; 1.00 g, 3.91 mmol) and Si–H-terminated PDMS (2.73 g, 0.14 mmol, $M_w = 2.00 \times 10^4$ g mol^{-1}, PDI = 1.60) in toluene (30 mL). After stirring for 24 h, the deep orange solution was precipitated into methanol (250 mL). The tacky orange gum was washed with methanol (3 × 200 mL) and dried under vacuum. Yield: 2.95 g (79 %); GPC: $M_n = 2.90 \times 10^4$ g mol^{-1}, PDI = 1.42; ^{1}H NMR (400 MHz, C_6D_6): $\delta = 0.28$ (s, 48 H; OSiMe_2O), 0.55 (s, 3 H; fcSiMeEt), 1.00 (br m, 2 H; fcSiMe(CH_2CH$_3$)), 1.17 (br m, 3 H; fcSiMe(CH$_2$$CH_3$)), 4.10 (s, 2 H; C_5H_4), 4.12 (s, 2 H; C_5H_4), 4.28 (br, 4 H; C_5H_4); ^{13}C NMR (100 MHz, C_6D_6): $\delta = -3.27$ (s, fcSiMe(CH$_2$CH$_3$)), −2.60 (s, fcSiMe(CH$_2$$CH_3$)), 1.35 (s, OSi$Me_2$O), 8.39 (s, fcSiMe($CH_2CH_3$)), 70.8 (s, ipso-$C_5H_4$), 71.7 (s, C_5H_4), 71.8 (s, C_5H_4), 73.8 (s, C_5H_4), 73.9 (s, C_5H_4); ^{29}Si{^{1}H} NMR (79.5 MHz, C_6D_6): $\delta = -21.8$ (s, OSiMe$_2$O), −4.3 (s, fcSiMeEt).

Synthesis of triblock copolymer PFMPS-*b*-PDMS-*b*-PFMPS (5): Karstedt's catalyst in xylenes (37 μL of a 0.3 % by weight solution) was added to a solution of **2** (R = Me, R′ = Ph; 1.00 g, 3.29 mmol) and Si–H-terminated PDMS (1.84 g, 0.10 mmol), $M_w = 2.00 \times 10^4$ g mol^{-1}, PDI = 1.60 (GPC) in toluene (20 mL). After stirring for 24 h, the resulting polymer was isolated by precipitation into methanol (ca. 200 mL) as a tacky orange gum. Yield: 2.10 g (73 %); GPC: $M_n = 3.00 \times 10^4$ g mol^{-1}, PDI = 1.38; ^{1}H NMR (400 MHz, C_6D_6): $\delta = 0.28$ (s, 46 H; OSiMe_2O), 0.75 (m, 3 H; fcSiMePh), 3.98–4.26 (m, 8 H; C_5H_4), 7.25 (br m, 3 H; fcSiMePh), 7.71 (br d, 2 H; fcSiMePh); ^{13}C NMR (100 MHz, C_6D_6): $\delta = -3.31$ (m, fcSiMePh), 1.35 (s, OSiMe_2O), 70.2 (m, ipso-C_5H_4), 71.9 (s, C_5H_4), 72.4 (s, C_5H_4), 74.2 (s, C_5H_4), 74.5 (s, C_5H_4), 129.3 (s, fcSiMePh), 134.6 (s, fcSiMePh), 138.8 (s, fcSiMePh); ^{29}Si NMR (79.5 MHz, C_6D_6): $\delta = -21.9$ (s, OSiMe$_2$O), −11.3 (s, fcSiMePh).

Preparation of samples for TEM and AFM: Micellar solutions were prepared by slowly adding *n*-hexane to a THF solution of triblock copolymer (ca. 100 mg mL^{-1}) until micellization had occurred. Subsequently, additional *n*-hexane was added until the solution contained 95 % (by volume) of *n*-hexane (total volume = 15 mL). The remainder of the THF was removed by dialyzing against pure *n*-hexane (M_w cutoff = 14 000 g mol^{-1}). Thin carbon films (ca. 5 Å) were grown on mica as a support, then 25 μL of a dilute solution of the block copolymer in hexane (ca. 0.2 %) was aerosol-sprayed onto the carbon film. Each carbon film was floated off the mica support in water and deposited onto a 300 mesh Gilder copper grid. The sample was air-dried before introduction into the electron microscope. No staining of the sample was necessary. Negative staining TEM experiments were conducted with TEM samples stained with about 10 μL of dodecatungstophosphoric acid ($H_3PO_4 \cdot 12\,WO_3 \cdot x\,H_2O$) dissolved in water to make a 0.3 wt % solution, followed by neutralization with a KOH solution of pH 6.5. Samples for AFM were prepared in an analogous manner to TEM samples, except that the solution was aerosol sprayed directly onto a freshly cleaved mica surface which was then mounted for imaging.

Acknowledgements

This research was supported by the Natural Sciences and Engineering Research Council of Canada (NSERC). R.R., K.T., and K.N.P. are grateful to NSERC for postgraduate scholarships and L.C. is grateful to the Ontario Government for a Ontario Graduate Scholarship. In addition, for the duration of the work M.A.W. is grateful to the Killam Foundation for a Fellowship and I.M. is grateful to NSERC for an E. W. R. Steacie Fellowship (1997–99), the University of Toronto for a McLean Fellowship (1997–2003), and the Ontario Government for a PREA award (1999).

[1] C. Price, *Pure Appl. Chem.* **1983**, *55*, 1563.
[2] M. Antionetti, C. Göltner, *Angew. Chem.* **1997**, *109*, 944; *Angew. Chem. Int. Ed. Engl.* **1997**, *36*, 910.
[3] J. P. Spatz, S. Mössmer, M. Möller, *Angew. Chem.* **1996**, *108*, 1673; *Angew. Chem. Int. Ed. Engl.* **1996**, *35*, 1510.
[4] For recent work on nonspherical micellar aggregates of organic block copolymers in solution, see: a) L. Zhang, A. Eisenberg, *Science* **1995**, *268*, 1728; b) L. Zhang, K. Yu, A. Eisenberg, *Science* **1996**, *272*, 1777; c) Y. Yu, A. Eisenberg, *J. Am. Chem. Soc.* **1997**, *119*, 8383; d) J. Tao, S. Stewart, G. Liu, M. Yang, *Macromolecules* **1997**, *30*, 2738; e) C. G. Göltner, B. Berton, E. Krämer, M. Antonietti, *Adv. Mater.* **1999**, *11*, 395; f) L. Chen, H. Shen, A. Eisenberg, *J. Phys. Chem. B* **1999**, *103*, 9488; g) Y.-Y. Won, H. T. Davis, F. S. Bates, *Science*, **1999**, *283*, 960; h) B. M. Discher, Y.-Y. Won, D. S. Ege, J. C.-M. Lee, F. S. Bates, D. E. Discher, D. A. Hammer, *Science*, **1999**, *284*, 1143; i) H. Shen, A. Eisenberg, *Macromolecules* **2000**, *33*, 2561; j) T. K. Bronich, A. M. Popov, A. Eisenberg, V. A. Kabanov, A. V. Kabanov, *Langmuir*, **2000**, *16*, 481; k) S. A. Jenekhe, X. L. Chen, *Science* **1998**, *72*, 864; l) H. Wang, H. H. Wang, V. S. Urban, K. C. Littrell, P. Thiyagarajan, L. Yu, *J. Am. Chem. Soc.* **2000**, *122*, 6855; m) G. Liu, J. Ding, L. Qiao, A. Guo, B. P. Dymov, J. T. Gleeson, H. K. Saijo, *Chem. Eur. J.* **1999**, *5*, 2740.
[5] Other routes to amphiphilic block copolymers include: Atom-transfer radical polymerization, see: a) T. E. Patten, J. H. Xia, T. Abernathy, K. Matyjaszewski, *Science* **1996**, *272*, 866; b) M. Cassebras, S. Pascual, A. Polton, M. Tardi, J.-P. Vairon, *Macromol. Rapid. Commun.* **1999**, *20*, 261; c) P. K. Tsolakis, E. G. Koulouri, J. K. Kallitsis, *Macromolecules* **1999**, *32*, 9054; for nitroxide-mediated free-radical polymerization, see: d) N. A. Listigovers, M. K. Georges, P. G. Odell, B. Keoshkerian, *Macromolecules* **1996**, *29*, 8992; for living cationic polymerization, see: e) E. Yoshida, A. Sugita, *J. Polym. Sci. Polym. Chem. A.* **1998**, *36*, 2059; for ring-opening metathesis polymerization, see: f) C. W. Bielawski, T. Morita, R. H. Grubbs, *Macromolecules* **2000**, *33*, 678.
[6] For recent intriguing examples of nanostructured materials based on block copolymers, see: a) C. C. Cummins, R. R. Schrock, R. E. Cohen, *Chem. Mater.* **1992**, *4*, 27; b) G. Liu, J. Ding, *Adv. Mater.* **1998**, *10*, 69; c) G. Liu, *Adv. Mater.* **1997**, *9*, 437; d) K. L. Wooley, *Chem. Eur. J.* **1997**, *3*, 1397; e) M. Moffitt, H. Vali, A. Eisenberg, *Chem. Mater.* **1998**, *10*, 1021; f) J. Spatz, S. Mössmer, M. Möller, M. Kocher, D. Neher, G. Wegner, *Adv. Mater.* **1998**, *10*, 473; g) L. Qi, H. Cölfen, M. Antonietti, *Angew. Chem.* **2000**, *112*, 617; *Angew. Chem. Int. Ed.* **2000**, *39*, 604; h) R. Ulrich, A. Du Chesne, M. Templin, U. Wiesner, *Adv. Mater.* **1999**, *11*, 141.
[7] For some recent work in the field of pluronics, see: a) C. Wu, T. Liu, H. White, B. Chu, *Langmuir* **2000**, *16*, 656; b) C. Olivia, H. Caldararu, A. A. Caragheorgheopol, *Langmuir* **1999**, *15*, 1891; c) K. Schillén, K. Bryskhe, Y. S. Mel′nikova, *Macromolecules* **1999**, *32*, 6885; d) Y. Chengzhong, Y. Yu, D. Zhao, *Chem. Commun.* **2000**, 575; e) A. Kyritsis, P. Polycarpos, S.-M. Mai, C. Booth, *Macromolecules*, **2000**, *33*, 4581.
[8] For insight into the factors which govern the self-assembly of triblock copolymers see, for example: a) V. Balsamo, R. Stadler, *Macromolecules* **1999**, *32*, 3994; b) O. F. Olaj, B. Neubauer, G. Zifferer, *Macromolecules* **1998**, *31*, 4350; c) S. Phan, G. H. Fredrickson, *Macromolecules* **1998**, *31*, 59; d) M. V. D. Banez, K. L. Robinson, S. P. Armes, *Macromolecules* **2000**, *33*, 451.
[9] For some recent work on non-spherical micelles obtained from amphiphilic triblock copolymers, see: a) G. Yu, A. Eisenberg, *Macromolecules* **1998**, *31*, 5546; b) S. Stewart, G. Liu, *Angew. Chem.* **2000**, *112*, 348; *Angew. Chem. Int. Ed.* **2000**, *39*, 340.
[10] G. ten Brinke, G. Hadziioannou, *Macromolecules* **1987**, *20*, 486.
[11] A. N. Semenov, J.-F. Joanny, A. R. Khokhlov, *Macromolecules* **1995**, *28*, 1066.
[12] A. Halperin, *Macromolecules* **1991**, *24*, 1418.
[13] Y. Wang, W. L. Mattice, D. H. Napper, *Macromolecules* **1992**, *25*, 4073.
[14] M. A. Hempenius, B. M. W. Langeveld-Voss, J. A. E. H. van Haare, R. A. J. Janssen, S. S. Sheiko, J. P. Spatz, M. Möller, E. W. Meijer, *J. Am. Chem. Soc.* **1998**, *120*, 2798.
[15] G. N. Tew, M. U. Pralle, S. I. Stupp, *J. Am. Chem. Soc.* **1999**, *121*, 9852.
[16] L. A. Schwegler, S. S. Sheiko, M. Möller, E. Fossum, K. Matyjaszewski, *Macromolecules* **1999**, *32*, 5901.
[17] Y. Heischkel, H.-W. Schmidt, *Macromol. Chem. Phys.* **1998**, *199*, 869.
[18] R. Rulkens, Y. Ni, I. Manners, *J. Am. Chem. Soc.* **1994**, *116*, 12121.
[19] Y. Ni, R. Rulkens, I. Manners, *J. Am. Chem. Soc.* **1996**, *118*, 4102.
[20] J. Massey, K. N. Power, I. Manners, M. A. Winnik, *J. Am. Chem. Soc.* **1998**, *120*, 9533.
[21] J. Massey, K. N. Power, I. Manners, M. A. Winnik, *Adv. Mater.* **1998**, *10*, 1559.
[22] R. Peterson, D. A. Foucher, B.-Z. Tang, A. J. Lough, N. P. Raju, J. E. Greedan, I. Manners, *Chem. Mater.* **1995**, *7*, 2045.
[23] M. MacLachlan, M. Ginzberg, N. Coombs, T. W. Coyle, N. P. Raju, J. E. Greedan, G. A. Ozin, I. Manners, *Science* **2000**, *287*, 1460.
[24] I. Manners, *Chem. Commun.* **1999**, 857.

[25] R. Resendes, A. Berenbaum, G. Stojevic, F. Jäkle, A. Bartole, F. Zamanian, G. Dubois, C. Hersom, K. Balmain, I. Manners, *Adv. Mater.* **2000**, *12*, 327.
[26] P. Gómez-Elipe, R. Resendes, P. M. Macdonald, I. Manners, *J. Am. Chem. Soc.* **1998**, *120*, 8348.
[27] K. Temple, F. Jäkle, J. B. Sheridan, I. Manners, *J. Am. Chem. Soc.* **2001**, in press.
[28] R. Resendes, J. A. Massey, H. Dorn, K. N. Power, M. A. Winnik, I. Manners, *Angew. Chem.* **1999**, *111*, 2738; *Angew. Chem. Int. Ed.* **1999**, *38*, 2570.
[29] a) J. Rasburn, R. Peterson, T. Jahr, R. Rulkens, I. Manners, G. J. Vancso, *Chem. Mater.* **1995**, *7*, 871; b) V. S. Papkov, M. V. Gerasimov, I. I. Dubovik, S. Sharma, V. V. Dementiev, K. H. Pannell, *Macromolecules* **2000**, *33*, 7107.
[30] a) S. J. Holder, R. C. Hiorns, N. A. J. M. Sommerdijk, S. J. Williams, R. G. Jones, R. J. M. Nolte, *Chem. Commun.* **1998**, *14*, 1445; b) N. A. J. M. Sommerdijk, S. J. Holder, R. C. Hiorns, R. G. Jones, R. J. M. Nolte, *Macromolecules* **2000**, *33*, 8289.
[31] Similar flower-like structures have been seen in materials obtained from the directed precipitation of calcium phosphate in the presence of amphiphilic block copolymers, see: M. Antonietti, M. Breulmann, G. Göltner, H. Cölfen, K. K. W. Wong, D. Walsh, S. Mann, *Chem. Eur. J.* **1998**, *4*, 2493.
[32] M. A. Hayat, S. E. Miller, *Negative Staining*, McGraw-Hill, New York, **1990**.
[33] S. N. Magonov, M.-H. Whangbo, *Surface Analysis with STM and AFM: Experimental and Theorectical Aspects of Image Analysis*, Wiley, Toronto, **1996**.
[34] K. Temple, J. A. Massey, Z. Chen, N. Vaidya, A. Berenbaum, M. D. Foster, I. Manners, *J. Inorg. Organomet. Polym.* **1999**, *9*, 189.
[35] R. Rulkens, A. J. Lough, I. Manners, S. R. Lovelace, C. Grant, W. E. Geiger, *J. Am. Chem. Soc.* **1996**, *118*, 12683.
[36] In parallel studies we have shown that crystallinity appears to play a similar role in the the formation of cylindrical rather than spherical micelles for the diblock copolymers PFDMS-*b*-PDMS and PFDMS-*b*-PI (PI = polyisoprene); see: J. A. Massey, K. Temple, L. Cao, Y. Rharbi, J. Raez, M. A. Winnik, I. Manners, *J. Am. Chem. Soc.* **2000**, *122*, 11577.

Received: August 31, 2000
Revised version: January 29, 2001 [F2703]

  0947-6539/01/0711-2424 $ 17.50+.50/0